Hopf Bifurcations Induced by SVC Controllers: A Didactic Example

Wei Gu [a,*] Federico Milano [b] Ping Jiang [a] Guoqing Tang [a]

[a] *SouthEast University, Dept. of Electrical Eng., NanJing, China*

[b] *University of Castilla - La Mancha, Dept. of Electrical Eng., Ciudad Real, 13071, Spain*

Abstract

This paper illustrates the effects of a static var compensator (SVC) device on the stability of a simple "single-machine dynamic-load" system. Firstly, the stability of the test system without SVC is investigated. The analysis is based on bifurcation diagrams, small signal stability analysis and time domain simulations. Without the SVC device, the system presents a saddle-node bifurcation. Then, static and dynamic analyses are repeated for the system with a SVC device located at the load bus. The SVC is able to improve system loadability but leads to a Hopf bifurcation. Finally a multi-parameter bifurcation analysis is presented to study the effect of system parameters on the Hopf bifurcation.

Key words: Voltage Collapse, Oscillatory Voltage Instability, Saddle-Node Bifurcation, Hopf Bifurcation, Bifurcation Control, SVC

1 Introduction

In recent years, voltage stability and voltage collapse phenomena have become more and more important issues in power system analysis and control [1,2]. It is well known that a proper modelling of power system devices, such as generators, loads, and regulators is fundamental to properly understand and reproduce voltage instability [3,4]. Furthermore, flexible AC transmission systems (FACTS) have been recognized as efficient solutions to improve power

* Corresponding author.
Email addresses: audrey.online@seu.edu.cn (Wei Gu), Federico.Milano@uclm.es (Federico Milano).

system stability [5,6]. This paper focuses on static var compensator (SVC) devices and their effects on voltage stability of power systems.

The bifurcation theory provides a set of mathematical techniques for nonlinear differential algebraic equations (DAE). Thus it is adequate for studying power electric systems that are typically modeled as a set of nonlinear DAE. In particular, the bifurcation theory is widely recognized as an effective tool to study voltage stability [7–10]. Relevant results on voltage stability are as follows: (i) Saddle-node bifurcations (SNB) lead to a monotonic voltage collapse [10]; (ii) Hopf bifurcations (HB) lead to undamped oscillations of bus voltages and likely to voltage collapse [8]; (iii) Limited-induced bifurcations, period-doubled bifurcations [9], blue-sky bifurcations [7] and chaos [8,11] are also routes to voltage instability phenomena. This paper focuses only on SNBs and HBs as these are the most common bifurcations that are induced by SVC devices.

In [12] and [13] it was introduced the concept of "bifurcation control", which in turns means that if one is able to "control" bifurcations, he is also able to avoid voltage instability and/or voltage collapse. The concept of bifurcation control is used in this paper for studying the effects of system parameters on the saddle-node and Hopf bifurcations. In particular, this paper discusses the effects of a SVC controller on HBs. Observe that, due to their flexibility and fast response, FACTS are currently used in real-world applications for bifurcation control [14].

This paper also shows that SVC and, more in general, FACTS controllers can lead to voltage instability phenomena. This has to be expected as control loops of FACTS regulators change the structure of the DAE of the system. Hence the need of properly tuning the parameters of FACTS controllers in order to avoid the occurrence of unexpected bifurcations.

In this paper, a didactic single-machine dynamic-load system [15,16] is used to illustrate the following issues: (i) Power systems generally have a maximum loading condition associated with a saddle-node bifurcation. (ii) The use of FACTS, in particular of a SVC, can improve the loadability of the system, thus avoiding the occurrence of the saddle-node bifurcation and the voltage collapse. (iii) SVC control parameters must be properly tuned to avoid the occurrence of Hopf bifurcations. This analysis leads to multi-parameter bifurcation diagrams similar to what was proposed in [17].

The paper is organized as follows. Section 2 provides outlines of voltage stability and bifurcation analysis. In particular, saddle-node and Hopf bifurcations are briefly described. Section 3 illustrates the single-machine dynamic-load example used in this paper. Static and dynamic simulations are provided in this section to illustrate the saddle-node bifurcation. Section 4 discusses the use

of a SVC controller as remedial action to avoid the saddle-node bifurcation. Static and dynamic simulations are also provided in this section to illustrate the effects of the SVC on the voltage stability and the birth of an unexpected Hopf bifurcation. Section 5 discusses the effects of a variety of system parameters on the Hopf bifurcation. Finally, in Section 6, conclusions are duly drawn.

2 Voltage Stability Outlines

Power electric systems can be represented as a set of dynamic algebraic equations (DAE) [18]:

$$\begin{aligned} \dot{x} &= f(x, y, p) \\ 0 &= g(x, y, p) \ , \end{aligned} \tag{1}$$

where ($f : \mathbb{R}^n \times \mathbb{R}^m \times \mathbb{R}^k \to \mathbb{R}^n$) is the vector of differential equations; $x \in \mathbb{R}^n$ is the vector of state variables associated with generators, loads and system controllers; ($g : \mathbb{R}^n \times \mathbb{R}^m \times \mathbb{R}^k \to \mathbb{R}^m$) is the vector of algebraic equations; $y \in \mathbb{R}^m$ is the vector of algebraic variables; and $p \in \mathbb{R}^k$ is the vector of parameters. It is assumed that algebraic variables can vary instantaneously, i.e. their transients are assumed to be "infinitely" fast.

Equations (1) can be linearized at an equilibrium point (x_0, y_0, p_0), as follows:

$$\begin{bmatrix} \Delta\dot{x} \\ 0 \end{bmatrix} = \begin{bmatrix} J_1 \ J_2 \\ J_3 \ J_4 \end{bmatrix} \begin{bmatrix} \Delta x \\ \Delta y \end{bmatrix} = [J] \begin{bmatrix} \Delta x \\ \Delta y \end{bmatrix} \ , \tag{2}$$

where J is the full system Jacobian matrix, and $J_1 = \partial f/\partial x|_0$, $J_2 = \partial f/\partial y|_0$, $J_3 = \partial g/\partial x|_0$ and $J_4 = \partial g/\partial y|_0$ are the Jacobian matrices of the differential and algebraic equations with respect to the state and algebraic variables, respectively. For the sake of completeness, the dimensions of all Jacobian matrices are given in the Appendix. If it is assumed that J_4 is nonsingular, the vector of algebraic variables Δy can be eliminated from (2), as follows:

$$\Delta\dot{x} = (J_1 - J_2 J_4^{-1} J_3)\Delta x = A\Delta x \ . \tag{3}$$

Thus the DAE can be implicitly reduced to a set of ordinary differential equations (ODE). Observe that if J_4 is singular, the model of the system have to be revised as the dynamics of some algebraic equations cannot be neglected [10]. Thus it is always possible to formulate a set of DAE for which J_4 is not singular.

In order to give a rigorous definition of the bifurcations discussed in this paper, let us assume that we can vary a scalar parameter λ ($\lambda \in \mathbb{R}$), being all other parameters constant. Then, let us define the vector of functions F as follows:

$$\dot{x} = F(x, \lambda) = f(x, y(x, \lambda), \lambda) \tag{4}$$

i.e. F is the set of differential equations where the algebraic variables y have been substituted for their explicit function of x and λ. Thus, one has:

$$A = \partial F / \partial x|_0 \tag{5}$$

Observe that, from the practical point of view, it is not necessary to know explicitly the function $y(x, \lambda)$ since the state matrix A can be computed from (3).

In this paper, bifurcation points are identified through the eigenvalue loci of the state matrix A. These bifurcations are the saddle-node bifurcation and the Hopf bifurcation. The definitions of these bifurcations are as follows.

Saddle-Node Bifurcation (SNB): a SNB point is an equilibrium point (x_0, λ_0) at which the state matrix presents one zero eigenvalue. SNB are associated with a pair of equilibrium points, one stable (s.e.p.) and one unstable (u.e.p.) that coalesce and disappear. The following transversality conditions hold:

(1) The state matrix A has a simple and unique eigenvalue with right and left eigenvectors v and w such that $Av = A^T w = 0$;
(2) $w^T \partial F / \partial \lambda|_0 = 0$;
(3) $w^T [\partial^2 F / \partial x^2] v \neq 0$.

Hopf Bifurcation (HB): a HB point is an equilibrium point (x_0, λ_0) at which the state matrix presents a complex conjugate pair of eigenvalues with zero real part. The following transversality conditions hold:

(1) The state matrix A has a simple pair of purely imaginary eigenvalues $\mu(\lambda_0) = \pm j\beta$ and no other eigenvalues with zero real part;
(2) $d\Re\{\mu(\lambda)/d\lambda|_0\} \neq 0$.

The HB gives a birth to a zero-amplitude limit cycle with initial period $T_0 = 2\pi/\beta$. If the limit cycle is stable the HB is "supercritical"; if the limit cycle is unstable the HB is "subcritical".

3 Single-Machine Dynamic-Load System

Figure 1 depicts a simple model of single-machine dynamic-load (SMDL) system. This didactic system was originally presented in [16,15] for voltage sta-

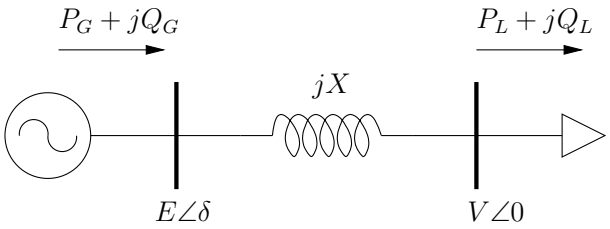

Fig. 1. One-line diagram of the single machine dynamic load (SMDL) system.

bility analysis. The following set of DAE is used to model the system:

$$\begin{aligned} \dot{\delta} &= \omega \\ \dot{\omega} &= \frac{1}{M}[P_m - P_G(V,\delta) - D\omega] \\ \dot{V} &= \frac{1}{\tau}[Q_L(V,\delta) - Q_d] \end{aligned} \tag{6}$$

and

$$\begin{aligned} P_G(V,\delta) &= \frac{EV}{X}\sin(\delta) \\ Q_L(V,\delta) &= -\frac{V^2}{X} + \frac{EV}{X}\cos(\delta)\ , \end{aligned} \tag{7}$$

where δ is the generator rotor angle; ω is the generator angular speed; M is the generator inertia constant; P_m is the mechanical power of prime mover; X is the line reactance; E is the generator voltage; D is the generator damping; τ is the voltage time constant of the dynamic load; and V is the bus voltage of the dynamic load.

The load power demand is $P_d + jQ_d$. For the sake of simplicity but without loss of generality, the resistance of the transmission line is neglected, i.e. $P_m = P_d$. Furthermore, it is assumed that the load, in steady-state conditions, has a constant power factor, i.e. $Q_d = kP_d$, where k is a given constant. Thus (6) can be simplified as follows:

$$\begin{aligned} \dot{\delta} &= \omega \\ \dot{\omega} &= \frac{1}{M}[P_d - \frac{EV}{X}\sin(\delta) - D\omega] \\ \dot{V} &= \frac{1}{\tau}[-kP_d - \frac{V^2}{X} + \frac{EV}{X}\cos(\delta)]\ , \end{aligned} \tag{8}$$

Observe that algebraic equations (7) have been eliminated from (8), thus leading to a set of ODE. Observe also that eliminating explicitly the algebraic variables is possible only in simple systems such as the one discussed in this

paper. The state matrix of (8) is as follows:

$$A = \left[\begin{array}{c|c|c} 0 & 1 & 0 \\ \hline -\frac{EV}{MX}\cos(\delta) & -\frac{D}{M} & -\frac{E}{MX}\sin(\delta) \\ \hline -\frac{EV}{\tau X}\sin(\delta) & 0 & \frac{1}{\tau X}[E\cos(\delta) - 2V] \end{array}\right] . \tag{9}$$

The active power demand P_d of the dynamic load is the parameter that can be varied, i.e. $\lambda = P_d$. All other system parameters are as follows: $M = 0.1$ s, $D = 0.1$, $X = 0.5$ p.u., $E = 1$ p.u., $k = 0.5$, and $\tau = 0.001$ s. Small signal stability analysis, bifurcation diagrams and time domain simulations are used to study bifurcations and stability as described in the following subsections.

3.1 Small Signal Stability Analysis

Figure 2 depicts the changes of relevant eigenvalues of the state matrix A as the active power demand P_d of the dynamic load increases. One eigenvalue crosses the imaginary axis for $P_d = 0.61805$ p.u., thus leading to a saddle-node bifurcation. The SNB point is:

$$(\delta_0, \omega_0, V_0, P_{d0}) = (0.5533, 0, 0.5881, 0.61805) .$$

Observe that, at the SNB point, the other two eigenvalues of the system are negative, thus the other system dynamics are stable.

3.2 Bifurcation Diagram

The stability of the system can be studied by means of the well known bifurcation diagrams. These diagrams are built by computing the equilibrium points of the system as one parameter varies, and then plotting any state variable as a function of that parameter. Figure 3 depicts the P_d-V curve for the SMDL system. As expected the "nose" is the SNB point and the load active power demand at the SNB point is $P_d = 0.61805$ p.u.

3.3 Time Domain Simulation

Figure 4 depicts the time domain simulation for a step change of P_d from 0.61 p.u. to 0.62 p.u. for $t = 2$ s. For $t \geq 4.751$ s, the system undergoes a voltage collapse induced by the saddle-node bifurcation. The voltage collapse is caused

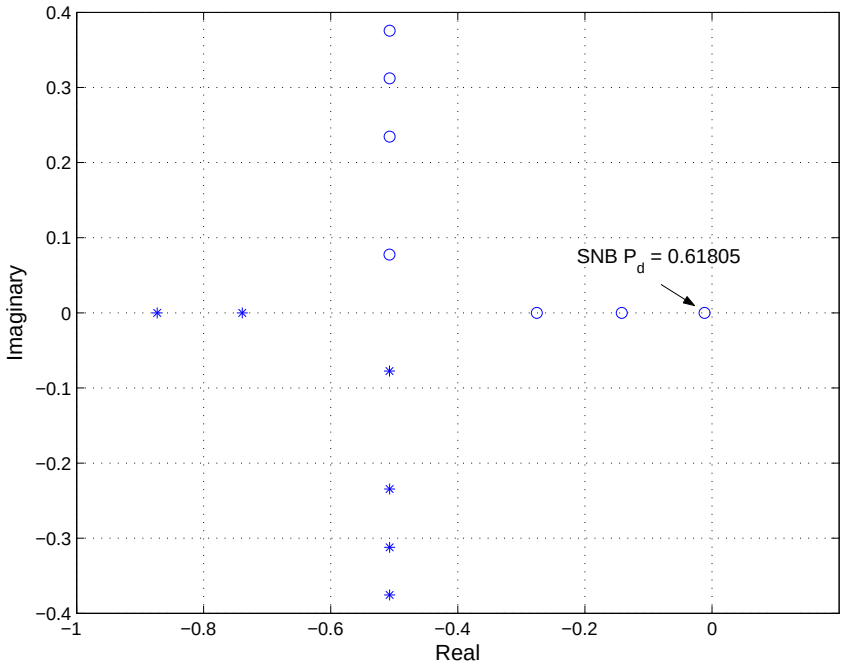

Fig. 2. SMDL system without SVC: Eigenvalue loci.

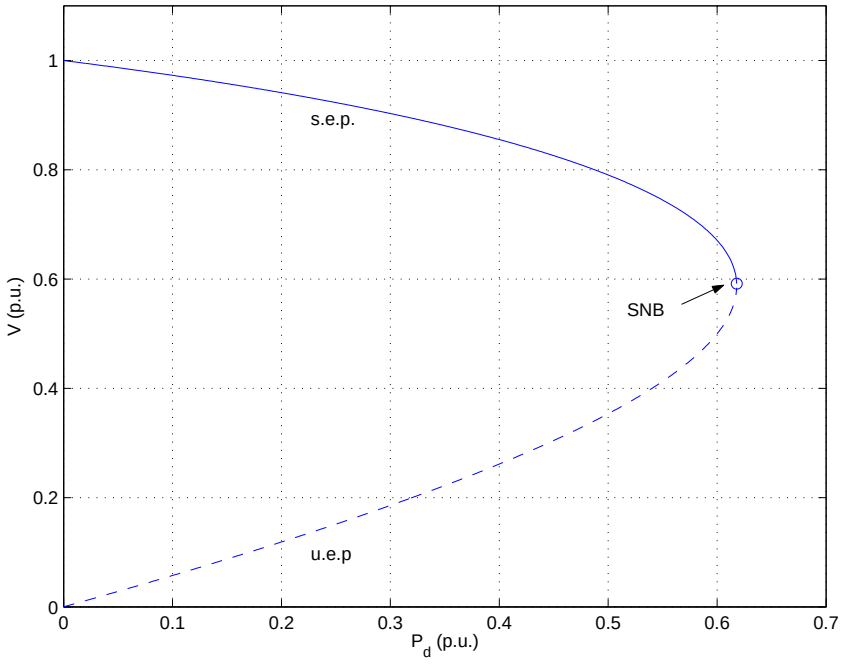

Fig. 3. SMDL system without SVC: Bifurcation diagram (P_d-V curve).

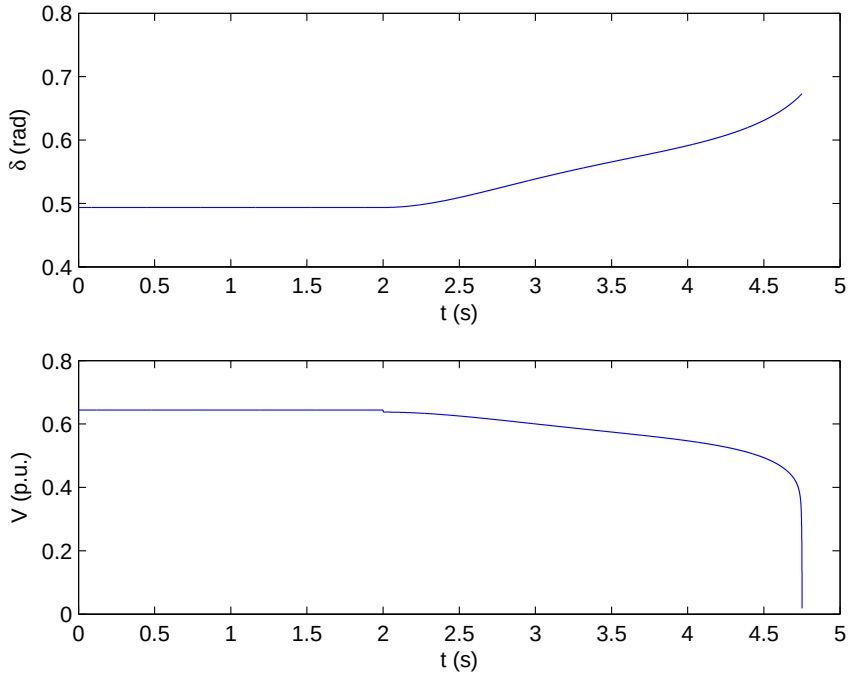

Fig. 4. SMDL system without SVC: Voltage collapse induced by a saddle-node bifurcation.

by the load dynamic. However, observe that, as a consequence of the voltage instability, also the generator rotor angle presents an unstable trajectory.

4 Single-Machine Dynamic-Load System with SVC

SVC devices are commonly used in power systems to control bus voltages and improve stability [5,14]. In this paper an SVC is used to control the voltage at the load bus of the SMDL system, as illustrated in Fig. 5.

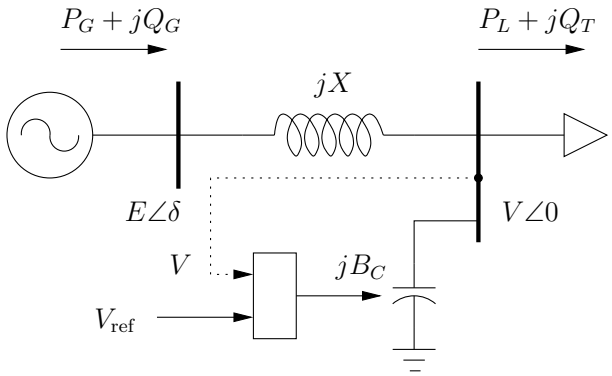

Fig. 5. One-line diagram of the SMDL system with SVC.

The total reactive power absorbed by the load and the SVC is as follows:

$$Q_T(V,\delta) = -\frac{V^2}{X} + \frac{EV}{X}\cos(\delta) + V^2 B_C \tag{10}$$

The SVC controller is modeled as a first order pure integrator, as depicted in Fig. 6.

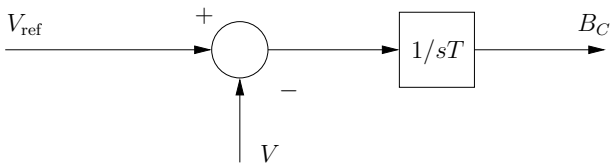

Fig. 6. SVC control scheme.

The resulting differential equations of the SMDL system with SVC are as follows:

$$\begin{aligned}
\dot{\delta} &= \omega \\
\dot{\omega} &= \frac{1}{M}[P_d - \frac{EV}{X}\sin(\delta) - D\omega] \\
\dot{V} &= \frac{1}{\tau}[-kP_d + V^2(B_C - \frac{1}{X}) + \frac{EV}{X}\cos(\delta)] \\
\dot{B}_C &= \frac{1}{T}(V_{\text{ref}} - V)\ ,
\end{aligned} \tag{11}$$

where B_C is the equivalent susceptance of the SVC; T and V_{ref} are the SVC time constant and reference voltage, respectively. In the following, unless otherwise specified, it is assumed that $T = 0.01$ s and $V_{\text{ref}} = 1.0$ p.u. Observe that also in this case it is possible to deduce the set of ODE, i.e. the algebraic variables can be explicitly expressed as a function of the state variables and the parameters.

The state matrix of (11) is as follows:

$$A = \left[\begin{array}{c|c|c|c}
0 & 1 & 0 & 0 \\ \hline
-\frac{EV}{MX}\cos(\delta) & -\frac{D}{M} & -\frac{E}{MX}\sin(\delta) & 0 \\ \hline
-\frac{EV}{\tau X}\sin(\delta) & 0 & \frac{1}{\tau X}[E\cos(\delta) - 2V + 2VB_CX] & \frac{V^2}{\tau} \\ \hline
0 & 0 & -\frac{1}{T} & 0
\end{array}\right]. \tag{12}$$

Small signal stability analysis, bifurcation diagrams and time domain simulations are used to study bifurcations and stability as described in the following subsections.

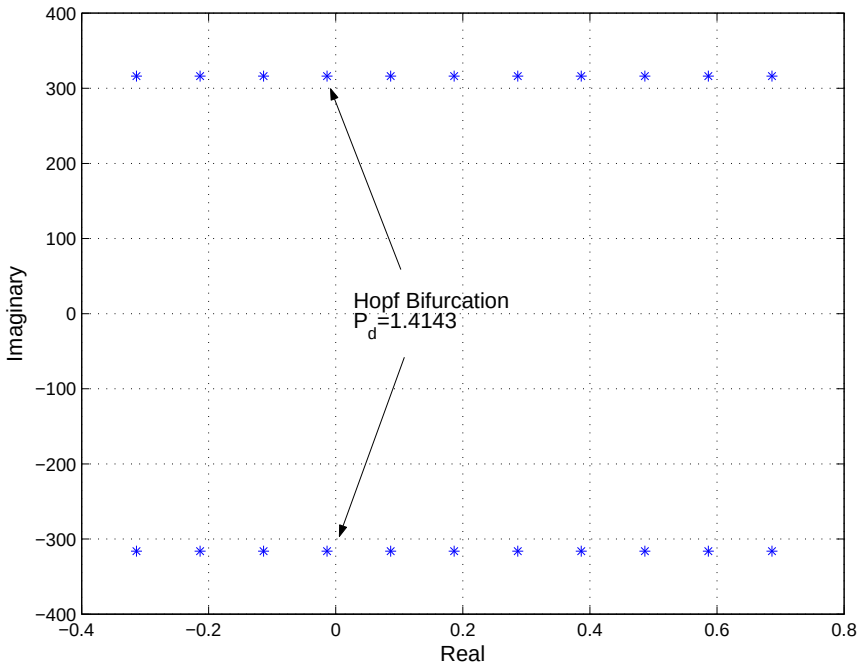

Fig. 7. SMDL system with SVC: Eigenvalue loci.

4.1 Small Signal Stability Analysis

Figure 7 depicts relevant eigenvalues for the SMDL system with SVC. A complex conjugate pair of eigenvalues crosses the imaginary axis for $P_d = 1.4143$, thus leading to a Hopf bifurcation. The HB point is:

$$(\delta_0, \omega_0, V_0, B_{C0}, P_{d0}) = (0.7855, 0, 1, 1.2930, 1.4143) \ .$$

4.2 Bifurcation Diagram

Also in this case, the parameter chosen for drawing the bifurcation diagram is the load demand P_d. Since the bus voltage is regulated, $V = V_{\text{ref}}$ at any equilibrium point. Thus, it is not relevant to plot the P_d-V curve. Figure 8 depicts the P_d-δ curve.

The solid and the dashed lines represent s.e.p. and u.e.p., respectively. Observe that the Hopf bifurcation point does not correspond to the point of maximum loadability of the system. However, as the parameter P_d increases over $P_d > 1.4143$ the system does not present stable equilibrium points. At $P_d = 2.0001$ p.u. a pair of complex eigenvalues with negative real part change

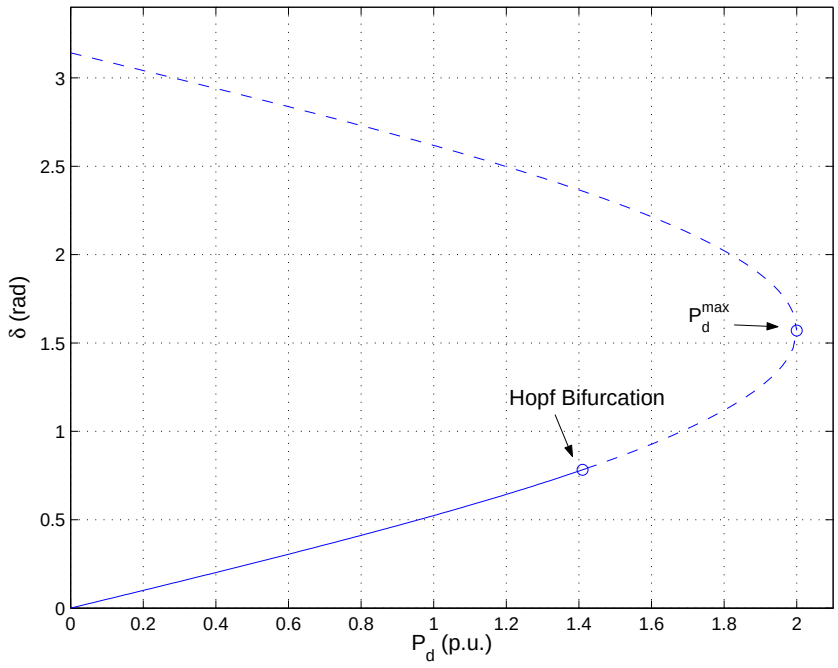

Fig. 8. SMDL system with SVC: Bifurcation diagram (P_d-δ curve).

to one positive and one negative real eigenvalues. This is the maximum loading condition corresponding to $\delta = \pi/2$, as follows:

$$(\delta_0, \omega_0, V_0, B_{C0}, P_{d0}) = (1.5708, 0, 1, 3, 2.0001) \ .$$

Observe that this maximum loading condition is an u.e.p., thus it is just a theoretical point as the system cannot reach it.

4.3 Time Domain Simulation

Figure 9 depicts the time domain simulation for a step change in P_d from 1.41 p.u. to 1.42 p.u. for $t = 2$ s. For $t > 2$ s the system does not present a stable equilibrium point and shows undamped oscillations (likely an unstable limit cycle), as expected from the P-δ curve of Section 4.2. For $t = 2.57$ s, the load voltage collapses. Note that, in this case, the generator angle shows an unstable trajectory only after the occurrence of the voltage collapse at the load bus.

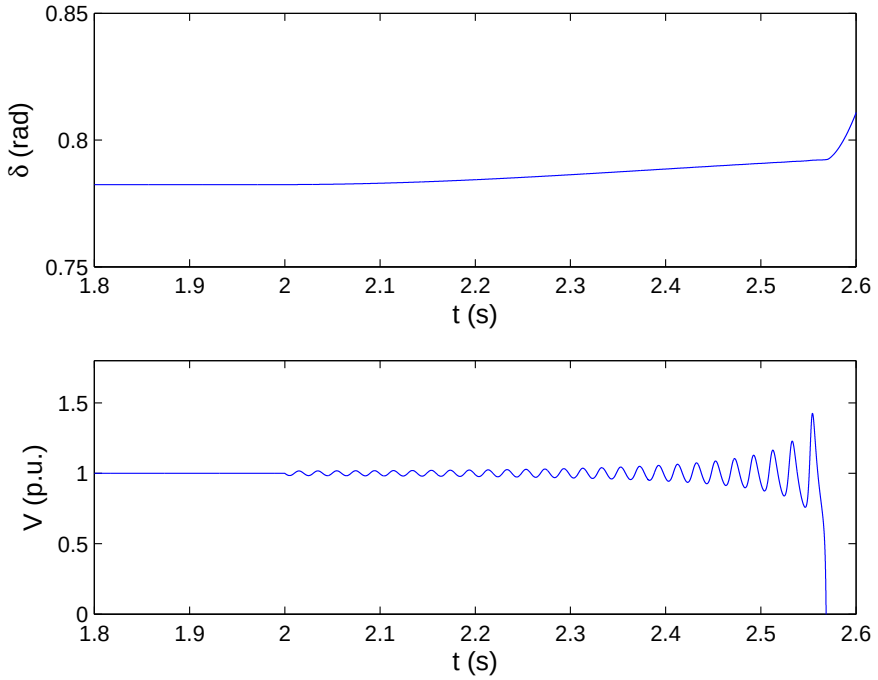

Fig. 9. SMDL system with SVC: Voltage collapse induced by Hopf bifurcation.

5 Multi-parameter Bifurcation Analysis

Sections 3 and 4 have considered a single scalar parameter, namely the load active power demand P_d. In this section, a multi-parameter bifurcation analysis method is carried out to study the effect of a variety of time constants, such as M, T and τ, on the value of the load active power demand P_d for which the HB occurs.

Two scenarios are discussed: (i) the effects of the rotor inertia M and the load time constant τ on the HB of the SMDL system, and (ii) the effects of the SVC regulator time constant T and the load time constant τ on the HB of the SMDL system. Final remarks are given in subsection 5.3.

5.1 Effects of M and τ on the HB of the SMDL system

Figures 10 illustrates the effects of different values of M and τ on the load active power P_{dHB}, which corresponds to the load level at which HBs occur. It is assumed that both M and τ vary in the range of $[0.1, 1.9]$ s. Figure 10 also depicts the loci of HB points corresponding to constant P_d values, for different combinations of M and τ values.

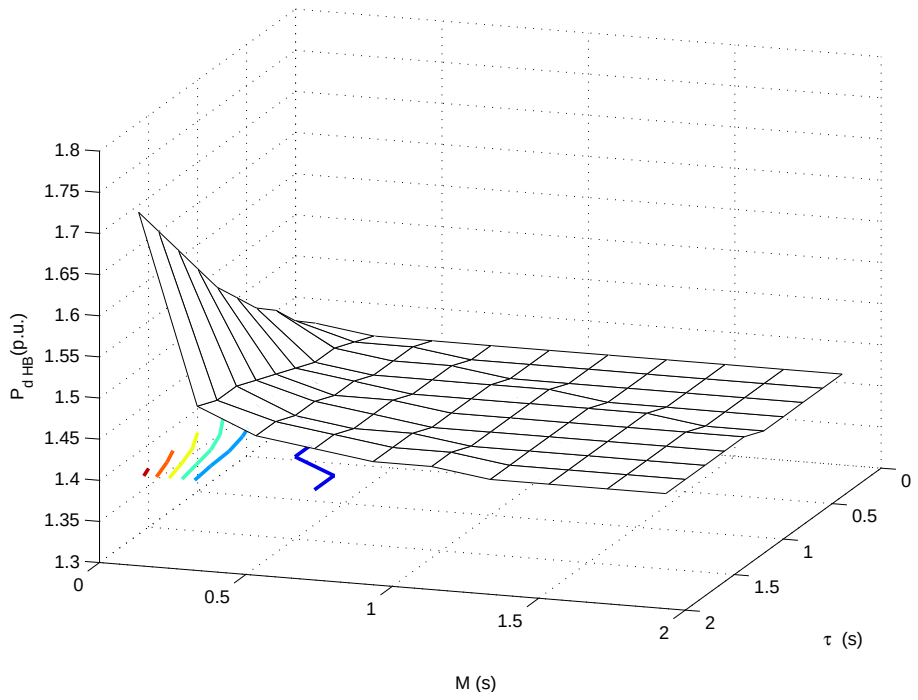

Fig. 10. Maximum load $P_d^{\max}$ parametrized with respect to generator inertia M and load time constant τ.

Results show that the system load P_{dHB} increases as time constant τ increases. On the other hand, the system load P_{dHB} decreases as the rotor inertia M increases.

Observe also that the variation of the rotor inertia M in the range of $[0.3, 1.9]$ has, in general, a small effect on the value of P_{dHB} at which the HB point occurs. The maximum load power demand for which a HB occurs is $P_{dHB}^{\max} = 1.7$ p.u., which corresponds to $M = 0.1$ s and $\tau = 1.9$ s.

5.2 Effects of T and τ on the HB of the SMDL system

Figures 11 illustrates the effects of different values of T and τ on the load active power P_{dHB}, which corresponds to the load level at which HBs occur. It is assumed that T and τ vary in the range of $[0.01, 0.1]$ s and $[0.1, 1.9]$ s, respectively. Figure 11 also depicts the loci of HB points corresponding to constant P_d values, for different combinations of T and τ values.

Results show that the system load P_{dHB} increases as time constants T decreases and τ increases. The maximum load power demand for which a HB occurs is $P_{dHB}^{\max} = 1.5$ p.u., which corresponds to $T = 0.04$ s and $\tau = 1.9$ s. Furthermore, the sensitivity of P_{dHB} with respect of T is noteworthy.

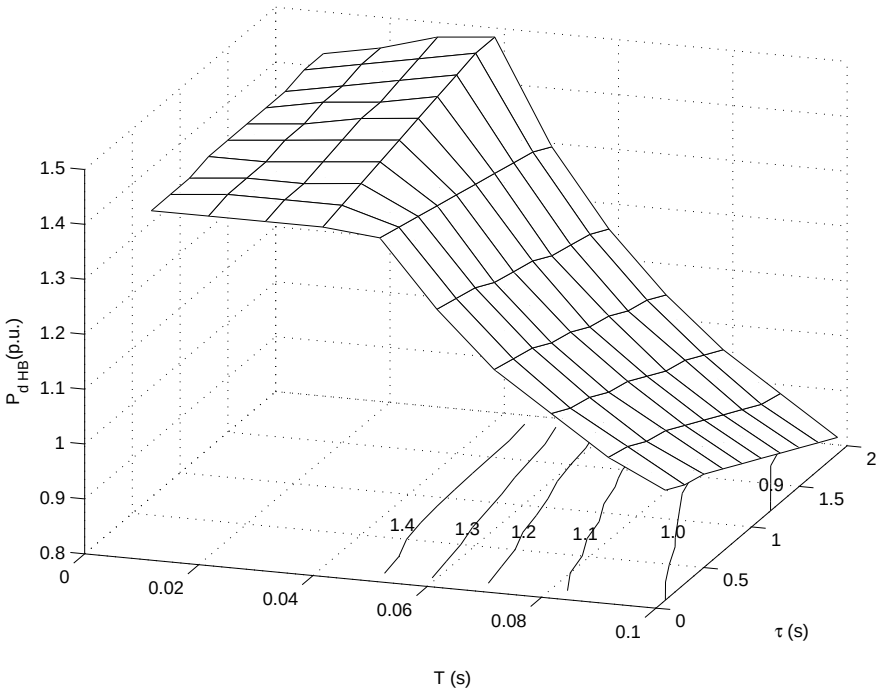

Fig. 11. Maximum load $P_d^{\max}$ parametrized with respect to SVC regulator time constant T and load time constant τ.

5.3 Remarks

Observe that, while generator inertias M cannot be regulated, the load and SVC dynamic response can be varied by means of adequate controls, thus leading to the possibility of an effective bifurcation control.

It is interesting to observe also that the best stability condition of the system, i.e. the highest load P_d for which a HB occurs, is obtained for the SVC time constant $T = 0.04$ s. Hence the need of properly tuning SVC control parameters.

As a final remark, note that the Hopf bifurcations is inherent ("robust") in this system. As a matter of fact, the HB is induced by SVC and load dynamics and cannot be eliminated by simply adjusting system parameters.

6 Discussion of Results and Conclusions

This paper has presented a didactic case study on the effects of a SVC controller on the stability of single-machine dynamic-load test system. The stability analysis is based on the well known bifurcation theory. The main results

obtained in this paper are summarized as follows:

(1) The SMDL without SVC presents a SNB point that limits the loadability of the system. If the load active power is increased over the SNB point, the system experiments a voltage collapse. If an SVC device is placed at the load bus, the loadability of the system can be increased.
(2) The use of the SVC device gives a birth to a new bifurcation, namely a Hopf bifurcation. This Hopf bifurcation cannot be removed by simply adjusting system parameters. However SVC and load dynamics can be coordinated so that the loadability of the system can be increased.

Due to the "robustness" of the Hopf bifurcation, the results obtained in this paper are valid in general and can be extended to more complex systems.

Future work will concentrate on studying different FACTS devices and their effects on the stability of the power systems and the synthesis of a general "bifurcation control" technique for FACTS controllers.

7 Acknowledgments

Federico Milano is partly supported by the Ministry of Science and Education of Spain through CICYT Project DPI-2003-01362 and by Junta de Comunidades de Castilla - La Mancha through project PBI-05-053.

Appendix

This Appendix provides the notation of all functions, variables and parameters used in this paper. For the sake of completeness, abbreviations are also provided in this section.

Functions

f	Differential equations ($f : \mathbb{R}^n \times \mathbb{R}^m \times \mathbb{R}^k \to \mathbb{R}^n$).
g	Algebraic equations ($g : \mathbb{R}^n \times \mathbb{R}^m \times \mathbb{R}^k \to \mathbb{R}^m$).
F	Differential equations ($F : \mathbb{R}^n \times \mathbb{R}^k \to \mathbb{R}^n$).

State Variables

x	Generic state variable vector ($x \in \mathbb{R}^n$).
δ	Generator rotor angle.
ω	Generator rotor speed.
V	Load bus voltage.
B_C	Susceptance of the SVC.

Algebraic Variables

y	Generic algebraic variable vector ($y \in \mathbb{R}^m$).
P_G	Generator active power.
Q_L	Load reactive power.
Q_d	Load reactive power demand.

Parameters

p	Generic parameter vector ($p \in \mathbb{R}^k$).
λ	Scalar parameter used for bifurcation analysis.
E	Generator regulated bus voltage.
M	Generator rotor inertia.
D	Generator damping.
P_m	Generator mechanical power.
X	Transmission line reactance.
P_d	Load active power demand.
P_{dHB}	Load active power demand corresponding to the HB point.
$P_d^{\max}$	Load active power demand corresponding to the SNB point.
k	Constant used for simulating a constant power factor load ($k = \tan\phi$).
τ	Load time constant.
V_{ref}	Voltage reference of the SVC controller.
T	SVC controller time constant.

Eigenvalues, Eigenvectors and Jacobian Matrices

All Jacobian matrices are computed at the equilibrium point (x_0, y_0, p_0). Dimensions are in parenthesis.

μ	Generic eigenvalue of the state matrix A.
β	Imaginary part of the eigenvalue complex pair at the HB point.

v	Right eigenvector of the state matrix A.
w	Left eigenvector of the state matrix A.
A	State matrix $(n \times n)$.
J	Full system Jacobian matrix $(n + m \times n + m)$.
J_1	Jacobian matrix $\partial f/\partial x$, $(n \times n)$.
J_2	Jacobian matrix $\partial f/\partial y$, $(n \times m)$.
J_3	Jacobian matrix $\partial g/\partial x$, $(m \times n)$.
J_4	Jacobian matrix $\partial g/\partial y$, $(m \times m)$.

Numbers

n	Number of state variables x.
m	Number of algebraic variables y.
k	Number of parameters p.

Abbreviations

DAE	Differential algebraic equations.
FACTS	Flexible AC transmission system.
HB	Hopf bifurcation.
ODE	Ordinary differential equations.
s.e.p.	Stable equilibrium point.
SMDL	Single machine dynamic load.
SNB	Saddle-node bifurcation.
SVC	Static var compensator.
u.e.p.	Unstable equilibrium point.

References

[1] C. W. Taylor, Power System Voltage Stability, McGraw-Hill, New York, 1994.

[2] T. Van Cutsem, C. Vournas, Voltage Stability of Electric Power Systems, Kluwer International Series in Engineering & Computer Science, Boston, 1998.

[3] I. Dobson, H.-D. Chiang, Towards a theory of voltage collapse in electric power systems, Systems and Control Letters 13 (1989) 253–262.

[4] D. J. Hill, Nonlinear Dyanmic Load Models with Recovery for Voltage Stability Studies, IEEE Trans. Power Systems 8 (1) (1993) 166–176.

[5] N. Mithulananthan, C. A. Cañizares, J. Reeve, G. J. Rogers, Comparison of PSS, SVC and STATCOM Controllers for Damping Power System Oscillations, IEEE Trans. Power Systems 18 (2) (2003) 786–792.

[6] N. G. Hingorani, Flexible AC Transmission, IEEE Spectrum (1993) 40–45.

[7] H. Wang, E. Abed, A. M. A. Hamdan, Bifurcations, Chaos, and Crises in Voltage Collapse of a Model Power System, IEEE Trans. on Circuits and Systems I: Fundamental Theory and Applications 41 (2) (1994) 294–302.

[8] V. Ajjarapu, B. Lee, Bifurcation Theory and its Application to Nonlinear Dynamical Phenomena in an Electrical Power System, IEEE Trans. Power Systems 7 (1) (1992) 424–431.

[9] W. Ji, V. Venkatasubramanian, Dynamics of a Minimal Power System: Invariant Tori and Quasi-Periodic Motions, IEEE Trans. on Circuits and Systems I: Fundamental Theory and Applications 42 (12) (1995) 981–1000.

[10] C. A. Cañizares, Voltage Stability Assessment: Concepts, Practices and Tools, Tech. rep., IEEE/PES Power System Stability Subcommittee, Final Document, available at http://www.power.uwaterloo.ca (Aug. 2002).

[11] A. S. Gugushvilli, G. N. Dalakishvili, N. M. Gomareli, V. M. Kekenadze, Bifurcation and Chaos in Power Systems, in: Proc. of Inter. conference on Control of Oscillation and Chaos, Russia, 1997, pp. 349–353.

[12] C. Guanrong, J. L. Moiola, H. O. Wang, Bifurcation Control: Theories, Methods, and Applications, International Journal of Bifurcation and Chaos 10 (3) (2000) 511–548.

[13] C. Guanrong, D. J. Hill, Y. Xinghuo, Bifurcation Control: Theory and Applications, Springer-Verlag, New York, 2003.

[14] C. A. Cañizares and M. Pozzi, FACTS Controllers Performance and Influence on Voltage Control in the Presence of Secondary Voltage Regulation, Tech. rep., CESI, RETE-A0/021456, Milan, Italy, 66 pages, available at http://www.power.uwaterloo.ca (Jun. 2000).

[15] C. A. Cañizares, Calculating Optimal System Parameters to Maximize the Distance to Saddle-Node Bifurcations, IEEE Trans. on Circuits and Systems I: Fundamental Theory and Applications 4 (3) (1998) 225–237.

[16] C. A. Cañizares, On Bifurcation Voltage Collapse and Load Modeling, IEEE Trans. Power Systems 10 (1) (1995) 512–522.

[17] A. A. P. Lerm, C. A. Cañizares, Multiparameter Bifurcation Analysis of the South Brazilian Power System, IEEE Trans. Power Systems 18 (2) (2003) 737–746.

[18] P. Kundur, Power System Stability and Control, McGraw Hill, New York, 1994.